Visualization of Uncertain Multivariate Data via Feature Confidence Level-Sets

Sudhanshu Sane[1], Tushar M. Athawale[1], and Chris R. Johnson[1]

[1]SCI Institute at University of Utah, USA

Abstract

Recent advancements in multivariate data visualization have opened new research opportunities for the visualization community. In this paper, we propose an uncertain multivariate data visualization technique called feature confidence level-sets. Conceptually, feature level-sets refer to level-sets of multivariate data. Our proposed technique extends the existing idea of univariate confidence isosurfaces to multivariate feature level-sets. Feature confidence level-sets are computed by considering the trait for a specific feature, a confidence interval, and the distribution of data at each grid point in the domain. Using uncertain multivariate data sets, we demonstrate the utility of the technique to visualize regions with uncertainty in relation to the specific trait or feature, and the ability of the technique to provide secondary feature structure visualization based on uncertainty.

CCS Concepts

• ***Human-centered computing*** → ***Scientific visualization;***

1. Introduction

Uncertain and multivariate data visualizations were viewed as major challenges during a visualization seminar at Daghstuhl in 2011, leading to a book [HCJ*14] providing an overview of the domain. Although scientific data extracted from computational simulations are often both uncertain and multivariate in nature, efforts to develop visualization techniques for these data types have been pursued independently due to the challenges involved. In this paper, we build upon a recent advancement in multivariate data visualization and extend an existing univariate uncertain data visualization technique to propose the first uncertain multivariate data visualization technique based on *feature level-sets*.

Recently, Jankowai and Hotz [JH20] proposed a technique for surface-based visualization of complex features in multivariate data called feature level-sets. They are the generalization of isosurfaces to multivariate data. Feature level-sets are surfaces in the spatial domain initialized by the distance field generated for a *trait* defined in attribute space. The "zero" feature level-set corresponds to the feature in the spatial domain that matches the trait exactly. In many cases, this feature is visualized using a small threshold distance to highlight the points in the domain that are closest to it.

In this paper, we extend *confidence isosurfaces*, an uncertain univariate data visualization technique [ZWK10], to multivariate data via feature level-sets. Specifically, we are interested in visualizing the uncertainty of the zero level-set. We contribute *feature confidence level-sets*, the generalization of confidence isosurfaces to multivariate data. Whereas feature level-sets compute a distance field based on the distribution of a function in the domain, feature confidence level-sets additionally consider the uncertainty of the function, represented in our study as a distribution at each grid point in the domain. Similar to feature level-sets, feature confidence level-sets can be defined using various distance metrics. To extract the zero level-set and the corresponding feature confidence level-sets, our approach utilizes distance fields computed in the spatial domain. We demonstrate our technique using uncertain multivariate synthetic, real, and simulation data sets.

2. Related Work

For comprehensive overviews, we refer readers to reports for uncertainty visualization [BHJ*14, JS03, PRJ11] and multivariate spatial data visualization [HTWL19]. In this section, we restrict our discussion to works most relevant to this study.

Two notable multivariate spatial data visualization efforts of the recent past are fiber surfaces and feature level-sets. Fiber surfaces, proposed by Carr et al. [CGT*15], are the generalization of isosurfaces to bivariate data and involve modifying the marching cubes algorithm. Parallelized implementations [KTCG16], direct volume rendering using higher-order interpolation schemes [WKI*17], uncertainty visualization [ZS21], and extensions to multivariate data [BRP*20] have been studied for fiber surfaces. Feature level-sets, as previously mentioned, are the generalization of isosurfaces to multivariate data and were proposed by Jankowai and Hotz [JH20]. Further studies of feature level-sets have focused on adapting the distance metric and smoothing of the distance field using Guassian kernels [NMC21], application to tensor data [JSJ*20], and use within visualization frameworks [JSS*20]. Another recent

DOI: 10.2312/evs.20211053

work, Hazarika et al. [HDSC19], first performed lossy in situ reduction via copula-based distribution models. Next, in response to bivariate data analysis queries, they visualized probability fields generated by distribution sampling of the stored data summary.

Several research studies have investigated quantification and visualization of uncertainty in univariate isosurfaces [GR04, PWH11, AJ19] and topology [AMY*20, YWM*20, FFST19]. Relevant to our work, Zehner et al. [ZWK10] proposed the confidence isosurfaces visualization technique for uncertain univariate data. Confidence isosurfaces are determined on the basis of a specific confidence interval percentage and provide an intuitive understanding by producing different shapes of isosurfaces due to uncertainty.

3. Our Method

We begin with a description of our uncertain multivariate data and the corresponding attribute space, followed by a discussion of trait specification, choice of distance metric, generation of feature level-sets, and finally, generation of feature confidence level-sets. Lastly, Figure 1 provides a notional example of the different steps involved to generate the level-sets and is referenced in Sections 3.4 and 3.5.

3.1. Uncertain Multivariate Data

From [JH20], general multivariate data are a set of scalar, vector, or tensor fields $\{F_1, F_2, ..., F_r\}$ in the domain $D \subset \mathbb{R}^3$, where $r \in \mathbb{N}$ and $r \geq 2$. Attribute space $\mathcal{A}$ is the combination of the field values and can further include derived quantities. The dimensionality of $\mathcal{A}$ is the combined dimensionality of all selected field values or derived quantities. Considering this definition of attribute space, multivariate data can be summarized as the mapping

$$f : D \to \mathcal{A} \subset R^n, \tag{1}$$

where n is the number of dimensions used to form attribute space. For uncertainty in each dimension i of attribute space, we assumed the normal distribution of values at each grid point in D and represented it using mean μ_i and standard deviation σ_i.

3.2. Trait Specification

Traits can be defined generally as arbitrary geometries in attribute space $\mathcal{A}$ whose equivalent counterparts in the spatial domain D are identified as features, i.e., $T \subset \mathcal{A}$. A trait can be of any dimension and structure, including points, intervals, lines, and volumes. For simplicity, we assume a limited definition of a trait T by considering intervals for each dimension i of attribute space $\mathcal{A}$

$$T = \forall i \, [L_i, U_i], \;\; L_i \leqslant U_i, \tag{2}$$

where L_i is the lower bound, and U_i is the upper bound of the interval for each dimension. As an example, in a visualization of $\mathcal{A}$ for $n = 2$ using a scatterplot, a trait by our definition would be a rectangular selection.

3.3. Distance Metric

The feature and feature confidence level-sets are extracted from distance fields. Our objective is to visualize the feature and feature confidence level-sets via the corresponding zero level-sets (see Sections 3.4 and 3.5, respectively). To achieve this, we computed distance fields using the Euclidean distance transformation (EDT) algorithm by Saito et al. [ST94] in the spatial domain. The field derived from the EDT algorithm is computed for each grid point in the spatial domain and encodes the minimum distance from a feature. A distance field computed in the spatial domain allows a domain information-guided selection of small threshold distances, whereas distance fields derived from attribute space can be harder to interpret due to dynamic ranges among attributes. In [JH20], the distance field is computed in attribute space to address empty features. In the event that a trait T results in an empty feature, our choice of distance metric would result in a constant distance field.

3.4. Feature Level-Sets

In general, a feature is defined as the pre-image of the trait T in the spatial domain with

$$f^{-1}(T) = \{x \in D | \; f(x) \in T\} \tag{3}$$

For our limited definition of a trait T and μ_i field of each dimension, a feature is defined as

$$f^{-1}(T) = \{x \in D | \; \forall i \; \mu_i(x) \cap [L_i, U_i] \neq \emptyset\} \tag{4}$$

To visualize the feature and its secondary structures, we performed three steps: First, for trait T, we computed a binary volume $bvolume_T$ (Figure 1b) to represent the absence or existence of the feature at a specific grid point

$$bvolume_T(x) = \begin{cases} 0, & \text{if } \forall i \; \mu_i(x) \cap [L_i, U_i] \neq \emptyset \\ 1, & \text{otherwise} \end{cases} \tag{5}$$

Second, we performed EDT using $bvolume_T$ as input to produce a distance field $distance_T$ (Figure 1c). As a final step, we computed feature level-set $FLS_{T,K}$ as the level-set of level K of the distance field such that

$$distance_T^{-1}(K) = \{x \in D \mid distance_T(x) = K\} \tag{6}$$

Here, the distance at each grid point is the minimum spatial dis-

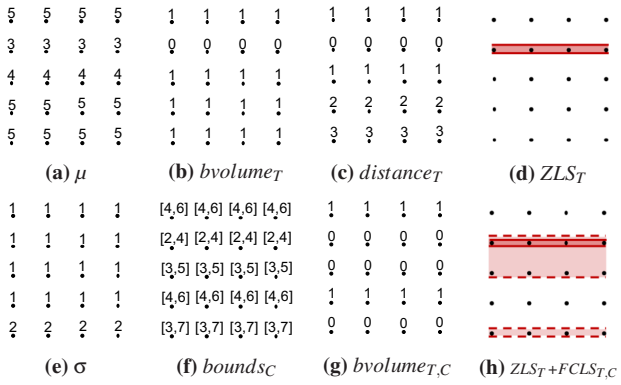

Figure 1: *A notional example showing the steps involved in generating the "zero" feature level-set ZLS_T (top row) and feature confidence level-set $FCLS_{T,C}$ (bottom row) for an uncertain univariate field represented using μ (a) and σ (e). For this example, we use trait $T = [2.5, 3.5]$ and confidence $C = 68\%$, i.e., $Z = 1$. $FCLS_{T,C}$ is computed using the $distance_{T,C}$ (not shown) field. Assuming a unit distance between adjacent grid points, $distance_{T,C}$ would be computed using $bvolume_{T,C}$ (g) as input and would appear equivalent for this example.*

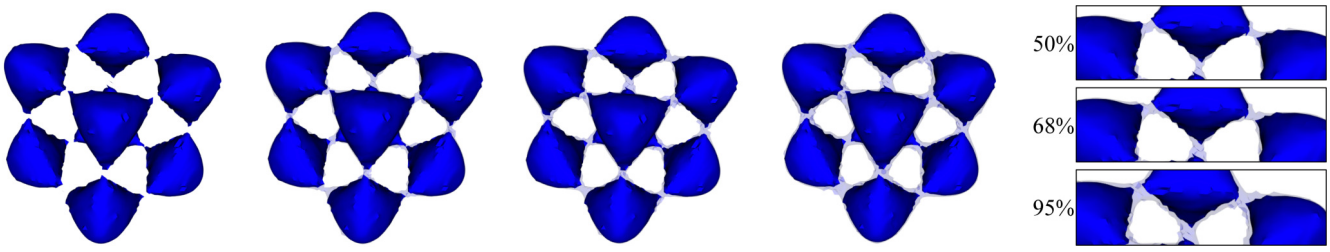

(a) ZLS_T **(b)** + $FCLS_{T,50\%}$ **(c)** + $FCLS_{T,68\%}$ **(d)** + $FCLS_{T,95\%}$ **(e)** *Comparison of* $FCLS_{T,C}$

Figure 2: *Visualization of the analytical tangle function [KHK*09] with a focus on uncertainty in linking regions between multiple blobs. We used* $T = [0, 62]$. *We use the "+" symbol to indicate augmentation to* ZLS_T. *For this data set, we found* $FCLS_{T,C}$ *(visualized as 25% opacity level-sets) are visible in the linking regions and form wider envelopes as the confidence interval increases from 50% (c) to 95% (e).*

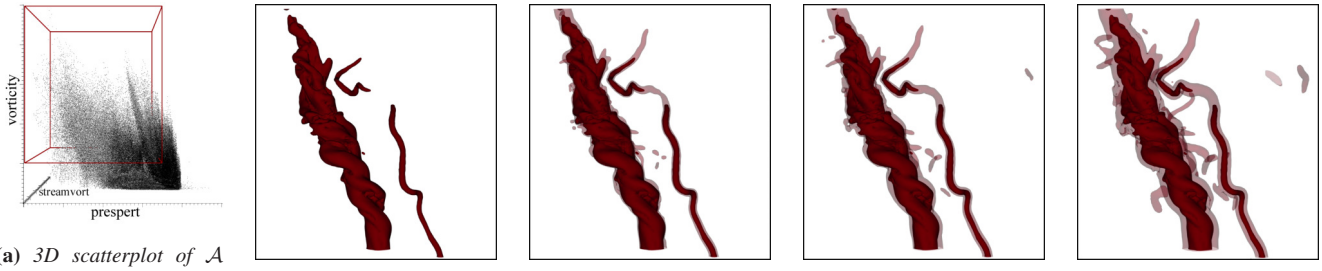

(a) *3D scatterplot of* $\mathcal{A}$ *and* T *(red cuboid).* **(b)** ZLS_T **(c)** + $FCLS_{T,50\%}$ **(d)** + $FCLS_{T,68\%}$ **(e)** + $FCLS_{T,95\%}$

Figure 3: *Visualization of EF-5 tornado vortices [Orf19] using vorticity, prespert and streamvort attributes. As in Figure 2,* $FCLS_{T,C}$ *formed wider envelopes as C increased. Importantly,* $FCLS_{T,C}$ *visualized vortical structures of interest in the vicinity of the primary tornado vortex.*

tance from $\forall i\ \mu_i(x) \cap [L_i, U_i] \neq \emptyset$. For $K = \varepsilon$, i.e., a small threshold value near zero, we refer to $FLS_{T,\varepsilon}$ as ZLS_T (Figure 1d).

3.5. Feature Confidence Level-Sets

Uncertainty in multivariate data can result in different shapes of ZLS_T. To assess the uncertainty, we visualized within which envelope the ZLS_T will lie for a certain confidence interval C. Similar to the steps we used to compute ZLS_T, to extract feature confidence level-sets $FCLS_{T,C}$, we first identified all the grid points that satisfy the trait T for confidence interval C. To achieve this, we used the method by Zehner et al. [ZWK10]. We used the Z-score, or the number of standard deviations from the mean a value would be, for a given confidence interval C, and then, for each dimension i, calculated $bounds_{i,C}$ (Figure 1f) as

$$bounds_{i,C}(x) = \forall i\ [\mu_i(x) - Z * \sigma_i(x),\ \ \mu_i(x) + Z * \sigma_i(x)] \tag{7}$$

Using $bounds_{i,C}$ and T, we computed $bvolume_{T,C}$ (Figure 1g)

$$bvolume_{T,C}(x) = \begin{cases} 0, & \text{if } \forall i\ bounds_{i,C}(x) \cap [L_i, U_i] \neq \emptyset \\ 1, & \text{otherwise} \end{cases} \tag{8}$$

Following the extraction of $bvolume_{T,C}$, we performed EDT to compute $distance_{T,C}$. Finally, we extracted the feature confidence level-set $FCLS_{T,C,K}$ as the level-set of level K of the distance field

$$distance^{-1}_{T,C}(K) = \{x \in D \mid distance_{T,C}(x) = K\} \tag{9}$$

Here, the distance at each grid point is the minimum spatial distance from $\forall i\ bounds_{i,C}(x) \cap [L_i, U_i] \neq \emptyset$. Given our objective of visualizing a single level-set extracted from $distance_{T,C}$ with $K = \varepsilon$, i.e., a small threshold value near zero, we refer to $FCLS_{T,C,\varepsilon}$ as simply $FCLS_{T,C}$ (Figure 1h).

4. Experimental Results

We demonstrated the use of feature confidence level-sets using five data sets. Specifically, we considered an analytical tangle function [KHK*09], an EF-5 Tornado [Orf19], an ethanediol molecule from a chemistry simulation, Red Sea and Gulf of Aden (RSGOA) eddy ensemble [STZ*20], and Earth's mantel convection [SYP17] data (see additional material). We defined between one to four traits per data set based on features of interest. In this study, each attribute was represented using a μ and σ field. For the RSGOA data set, we computed μ and σ fields using 20 ensemble members. For other data sets, we synthetically estimated σ for each scalar field of the multivariate data at each grid point by sampling the local neighborhood. To evaluate our technique, we visualized the ZLS_T both in isolation and augmented with $FCLS_{T,C}$. When visualized together, the ZLS_T is shown using an opaque level-set, and the $FCLS_{T,C}$ is shown using a level-set colored with the same hue and 25% opacity. We used VisIt [CBW*12] to extract and render smooth level-sets using the pseudocolor plot and isosurface operator.

Across all data sets, the shape of $FCLS_{T,C}$ corresponded to the uncertainty of the data in the spatial domain. For example, for the analytical tangle function where uncertainty is higher near the links between the blobs for the trait specified, we found, comparing Figures 2c and 2d, the $FCLS_{T,C}$ envelope expanded between the links in response to increasing the value of C, but not significantly on the exterior of the blob surface. For the Tornado data set, we specify a trait using three attributes related to vorticity, including negative pressure pertubation (prespert) values that are associated with the updraft rotational mechanics of an evolving tornado to extract the primary vortex. $FCLS_{T,C}$ visualize weaker vortices in proximity to the primary vortex in Figure 3e. Such visualizations could be use-

(a) *2D scatterplot of $\mathcal{A}$ and traits. We use $T = \{T_A, T_B\}$.*

(b) ZLS_T **(c)** + $FCLS_{T,50\%}$ **(d)** + $FCLS_{T,68\%}$

Figure 4: *Visualization of anticyclonic (T_A, red) and cyclonic (T_B, blue) eddies in the Gulf of Aden and part of the Red Sea using the derived attributes of vorticity magnitude and the z-component of curl. For this ensemble data set [STZ*20], the uncertainty resulted in $FCLS_{T,C}$ visualizing additional tracks and regions with eddies. The orange boxes in 4c and 4d highlight one such example.*

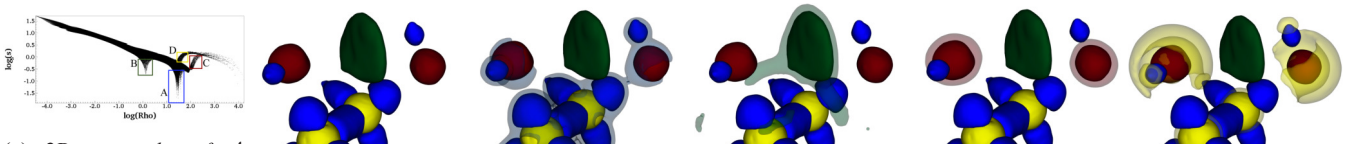

(a) *2D scatterplot of $\mathcal{A}$ and traits. We use $T = \{T_A, T_B, T_C, T_D\}$.*

(b) ZLS_T **(c)** + $FCLS_{T_A,68\%}$ **(d)** + $FCLS_{T_B,68\%}$ **(e)** + $FCLS_{T_C,68\%}$ **(f)** + $FCLS_{T_D,68\%}$

Figure 5: *The covalent bonds (T_A, blue), non-covalent bond (T_B, green), oxygen atoms (T_C, red), and carbon atoms (T_D, yellow) of an ethanediol molecule are visualized using the electron density (Rho) and reduced gradient (s) attributes. These attributes are related exponentially in regions where no chemical interaction occurs and we selected our traits accordingly. In this case, we found $FCLS_{T,C}$ collectively visualized elements of the topological structure of the molecule.*

ful in visualizing vortex merges during the formation of a multiple vortex tornado [Orf19].

For the RSGOA data, we visualized anticyclonic (red isosurfaces) and cyclonic (blue isosurfaces) eddies in Figure 4. Using the μ field to compute ZLS_T for the two specified traits (Figure 4a) reveals regions where large eddies in the Gulf of Aden and eddy tracks in the Red Sea exist, as well as the type of eddy in Figure 4b. To investigate the uncertainty of outcomes across ensemble members, the μ and σ fields are utilized to compute $FCLS_{T,C}$ for 50% and 68% confidence intervals. Besides showing larger regions of eddys in the Gulf of Aden, $FCLS_{T,C}$ visualizes the possible existence of additional eddy tracks in the Red Sea across ensemble members for the specific trait selection, which is not seen in the ZLS_T derived from the mean fields. Figures 4c and 4d are annotated to highlight an example of possible eddy tracks.

In the ethanediol data set, electron density and reduced gradient are related exponentially in regions where no chemical interactions occur (main separating axis of the scatterplot in Figure 5a). Our trait selections in attribute space are off this axis and correspond to regions with significant chemical interactions. In this case, we found $FCLS_{T,C}$ of individual traits visualized the boundaries of non-chemical interactivity for each feature. Figures 5c and 5d show $FCLS_{T,C}$ for the covalent and non-covalent bond form enclosing structures primarily around the respective features. Similarly, in Figures 5e and 5f, $FCLS_{T,C}$ of each trait are observed in regions of influence of each atom, conveying the proximity of the traits in attribute space and the uncertainty in the data. Figure 5e contains occluded $FCLS_{T_C,C}$ on the inside of each carbon atom (yellow). Overall, by leveraging the information pertaining to field distribution (μ, σ), $FCLS_{T,C}$ provided secondary structure visualization based on uncertainty.

5. Future Work and Conclusion

In this paper, we proposed feature confidence level-sets and demonstrated their use for uncertain multivariate data visualization. Several opportunities, however, remain for future work in this direction. Similar to feature level-sets [JH20], addressing discernibility and intuitive trait specification interfaces for high-dimensional data with uncertainty are challenges for feature confidence level-sets. Considering the impact of the source of uncertainty and representation of the multivariate data, we plan to investigate the use of feature confidence level-sets on scientific data from lossy compressors such as ZFP [Lin14], as well as parametric and non-parametric density models. Further, we aim to pursue visualization of interquartile ranges for uncertain multivariate data and performance optimizations that can be introduced to render implicit feature and feature confidence level-sets.

Overall, we contributed a technique to visualize uncertain multivariate data based on confidence isosurfaces and feature level-sets. Our study demonstrated the ability of the approach to visualize regions of uncertainty in relation to a specific trait or feature, and visualize secondary feature structures based on uncertainty.

Acknowledgment

The authors acknowledge current research support provided in part by the Intel Graphics and Visualization Institutes of XeLLENCE, the National Institutes of Health under grant numbers P41 GM103545 and R24 GM136986 and the Department of Energy under grant number DE- FE0031880.

References

[AJ19] ATHAWALE T., JOHNSON C. R.: Probabilistic asymptotic decider for topological ambiguity resolution in level-set extraction for uncertain 2D data. *IEEE Transactions on Visualization and Computer Graphics 25*, 1 (2019), 1163–1172. doi:10.1109/TVCG.2018.2864505. 2

[AMY*20] ATHAWALE T., MALJOVEC D., YAN L., JOHNSON C., PASCUCCI V., WANG B.: Uncertainty visualization of 2D morse complex ensembles using statistical summary maps. *IEEE Transactions on Visualization and Computer Graphics* (2020), 1–1. doi:10.1109/TVCG.2020.3022359. 2

[BHJ*14] BONNEAU G.-P., HEGE H.-C., JOHNSON C. R., OLIVEIRA M. M., POTTER K., RHEINGANS P., SCHULTZ T.: *Overview and State-of-the-Art of Uncertainty Visualization*. Springer London, London, 2014, pp. 3–27. doi:10.1007/978-1-4471-6497-5_1. 1

[BRP*20] BLECHA C., RAITH F., PRÄGER A. J., NAGEL T., KOLDITZ O., MASSMANN J., RÖBER N., BÖTTINGER M., SCHEUERMANN G.: Fiber surfaces for many variables. *Computer Graphics Forum 39*, 3 (2020), 317–329. doi:10.1111/cgf.13983. 1

[CBW*12] CHILDS H., BRUGGER E., WHITLOCK B., MEREDITH J. S., AHERN S., PUGMIRE D., BIAGAS K., MILLER M. C., HARRISON C., WEBER G. H., KRISHNAN H., FOGAL T., SANDERSON A. R., GARTH C., BETHEL E. W., CAMP D., RÜBEL O., DURANT M., FAVRE J. M., NAVRÁTIL P. A.: Visit. In *High Performance Visualization - Enabling Extreme-Scale Scientific Insight*. CRC Press, 2012. doi:10.1201/b12985-21. 3

[CGT*15] CARR H., GENG Z., TIERNY J., CHATTOPADHYAY A., KNOLL A.: Fiber surfaces: Generalizing isosurfaces to bivariate data. *Computer Graphics Forum 34*, 3 (2015), 241–250. doi:10.1111/cgf.12636. 1

[FFST19] FAVELIER G., FARAJ N., SUMMA B., TIERNY J.: Persistence atlas for critical point variability in ensembles. *IEEE Transactions on Visualization and Computer Graphics 25*, 1 (2019), 1152–1162. doi:10.1109/TVCG.2018.2864432. 2

[GR04] GRIGORYAN G., RHEINGANS P.: Point-based probabilistic surfaces to show surface uncertainty. *IEEE Transactions on Visualization and Computer Graphics 10*, 5 (2004), 564–573. doi:10.1109/TVCG.2004.30. 2

[HCJ*14] HANSEN C. D., CHEN M., JOHNSON C. R., KAUFMAN A. E., HAGEN H.: *Scientific Visualization: Uncertainty, Multifield, Biomedical, and Scalable Visualization*. Springer Publishing Company, Incorporated, 2014. doi:10.1007/978-1-4471-6497-5. 1

[HDSC19] HAZARIKA S., DUTTA S., SHEN H., CHEN J.: Codda: A flexible copula-based distribution driven analysis framework for large-scale multivariate data. *IEEE Transactions on Visualization and Computer Graphics 25*, 1 (2019), 1214–1224. doi:10.1109/TVCG.2018.2864801. 1

[HTWL19] HE X., TAO Y., WANG Q., LIN H.: Multivariate spatial data visualization: a survey. *Journal of Visualization 22*, 5 (2019), 897–912. doi:10.1007/s12650-019-00584-3. 1

[JH20] JANKOWAI J., HOTZ I.: Feature level-sets: Generalizing iso-surfaces to multi-variate data. *IEEE Transactions on Visualization and Computer Graphics 26*, 2 (2020), 1308–1319. doi:10.1109/TVCG.2018.2867488. 1, 2, 4

[JS03] JOHNSON C. R., SANDERSON A. R.: A next step: Visualizing errors and uncertainty. *IEEE Computer Graphics and Applications 23*, 5 (2003), 6–10. doi:10.1109/MCG.2003.1231171. 1

[JSJ*20] JANKOWAI J., SKÅNBERG R., JÖNSSON D., YNNERMAN A., HOTZ I.: Tensor volume exploration using attribute space representatives, Nov 2020. doi:10.31219/osf.io/qu8rz. 1

[JSS*20] JÖNSSON D., STENETEG P., SUNDÉN E., ENGLUND R., KOTTRAVEL S., FALK M., YNNERMAN A., HOTZ I., ROPINSKI T.: Inviwo — a visualization system with usage abstraction levels. *IEEE Transactions on Visualization and Computer Graphics 26*, 11 (2020), 3241–3254. doi:10.1109/TVCG.2019.2920639. 1

[KHK*09] KNOLL A., HIJAZI Y., KENSLER A., SCHOTT M., HANSEN C., HAGEN H.: Fast ray tracing of arbitrary implicit surfaces with interval and affine arithmetic. *Computer Graphics Forum 28*, 1 (2009), 26–40. doi:10.1111/j.1467-8659.2008.01189.x. 3

[KTCG16] KLACANSKY P., TIERNY J., CARR H., GENG Z.: Fast and exact fiber surfaces for tetrahedral meshes. *IEEE Transactions on Visualization and Computer Graphics 23*, 7 (2016), 1782–1795. doi:10.1109/TVCG.2016.2570215. 1

[Lin14] LINDSTROM P.: Fixed-rate compressed floating-point arrays. *IEEE Transactions on Visualization and Computer Graphics 20*, 12 (2014), 2674–2683. doi:10.1109/TVCG.2014.2346458. 4

[NMC21] NGUYEN D. B., MONICO R., CHEN G.: A visualization framework for multi-scale coherent structures in taylor-couette turbulence. *IEEE Transactions on Visualization and Computer Graphics 27*, 02 (2021), 902–912. doi:10.1109/TVCG.2020.3028892. 1

[Orf19] ORF L.: A violently tornadic supercell thunderstorm simulation spanning a quarter-trillion grid volumes: Computational challenges, i/o framework, and visualizations of tornadogenesis. *Atmosphere 10*, 10 (2019). doi:10.3390/atmos10100578. 3, 4

[PRJ11] POTTER K., ROSEN P., JOHNSON C. R.: From quantification to visualization: A taxonomy of uncertainty visualization approaches. In *IFIP Working Conference on Uncertainty Quantification* (2011), Springer, pp. 226–249. doi:10.1007/978-3-642-32677-6_15. 1

[PWH11] PÖTHKOW K., WEBER B., HEGE H.-C.: Probabilistic marching cubes. *Computer Graphics Forum 30*, 3 (2011), 931–940. doi:10.1111/j.1467-8659.2011.01942.x. 2

[ST94] SAITO T., TORIWAKI J.-I.: New algorithms for Euclidean distance transformation of an n-dimensional digitized picture with applications. *Pattern Recognition 27*, 11 (1994), 1551–1565. doi:10.1016/0031-3203(94)90133-3. 2

[STZ*20] SANIKOMMU S., TOYE H., ZHAN P., LANGODAN S., KROKOS G., KNIO O., HOTEIT I.: Impact of atmospheric and model physics perturbations on a high-resolution ensemble data assimilation system of the red sea. *Journal of Geophysical Research: Oceans 125*, 8 (2020). doi:10.1029/2019JC015611. 3, 4

[SYP17] SHAHNAS M., YUEN D., PYSKLYWEC R.: Mid-mantle heterogeneities and iron spin transition in the lower mantle: Implications for mid-mantle slab stagnation. *Earth and Planetary Science Letters 458* (2017), 293–304. doi:https://doi.org/10.1016/j.epsl.2016.10.052. 3

[WKI*17] WU K., KNOLL A., ISAAC B. J., CARR H., PASCUCCI V.: Direct multifield volume ray casting of fiber surfaces. *IEEE Transactions on Visualization and Computer Graphics 23*, 1 (2017), 941–949. doi:10.1109/TVCG.2016.2599040. 1

[YWM*20] YAN L., WANG Y., MUNCH E., GASPAROVIC E., WANG B.: A structural average of labeled merge trees for uncertainty visualization. *IEEE Transactions on Visualization and Computer Graphics 26*, 1 (2020), 832–842. doi:10.1109/TVCG.2019.2934242. 2

[ZS21] ZHENG B., SADLO F.: Uncertainty in continuous scatterplots, continuous parallel coordinates, and fibers. *IEEE Transactions on Visualization and Computer Graphics 27*, 2 (2021), 1819–1828. doi:10.1109/TVCG.2020.3030466. 1

[ZWK10] ZEHNER B., WATANABE N., KOLDITZ O.: Visualization of gridded scalar data with uncertainty in geosciences. *Computers and Geosciences 36*, 10 (2010), 1268–1275. doi:https://doi.org/10.1016/j.cageo.2010.02.010. 1, 2, 3